Received: 30 May 2022 | Accepted: 20 September 2022

DOI: 10.1097/HC9.0000000000000008

ORIGINAL ARTICLE

OPEN

Hepatic MCPIP1 protein levels are reduced in NAFLD patients and are predominantly expressed in cholangiocytes and liver endothelium

Natalia Pydyn[1] | Justyna Kadluczka[1,2] | Piotr Major[3] | Tomasz Hutsch[4,5] | Kinga Belamri[5] | Piotr Malczak[3] | Dorota Radkowiak[3] | Andrzej Budzynski[3] | Katarzyna Miekus[1] | Jolanta Jura[1] | Jerzy Kotlinowski[1]

[1]Department of General Biochemistry, Faculty of Biochemistry, Biophysics and Biotechnology, Jagiellonian University, Krakow, Poland

[2]Department of Neuropsychopharmacology, Maj Institute of Pharmacology Polish Academy of Sciences, Krakow, Poland

[3]2nd Department of General Surgery, Jagiellonian University Medical College, Krakow, Poland

[4] Department of Pathology and Veterinary Diagnostics, Institute of Veterinary Medicine, Warsaw University of Life Sciences, Warsaw, Poland

[5]Veterinary Diagnostic Laboratory ALAB Bioscience, Warsaw, Poland

Correspondence
Jerzy Kotlinowski, Gronostajowa Street 7, Krakow 30-387, Poland.
Email: j.kotlinowski@uj.edu.pl

Funding information
This work was supported by research grants from the National Science Centre, Poland, no. 2015/19/D/NZ5/00254 and 2017/27/B/NZ5/01440 to JeKo.

Abstract

Background and Aims: NAFLD is characterized by the excessive accumulation of fat in hepatocytes. NAFLD can range from simple steatosis to the aggressive form called NASH, which is characterized by both fatty liver and liver inflammation. Without proper treatment, NAFLD may further progress to life-threatening complications, such as fibrosis, cirrhosis, or liver failure. Monocyte chemoattractant protein-induced protein 1 (MCPIP1, alias Regnase 1) is a negative regulator of inflammation, acting through the cleavage of transcripts coding for proinflammatory cytokines and the inhibition of NF-κB activity.

Methods: In this study, we investigated MCPIP1 expression in the liver and peripheral blood mononuclear cells (PBMCs) collected from a cohort of 36 control and NAFLD patients hospitalized due to bariatric surgery or primary inguinal hernia laparoscopic repair. Based on liver histology data (hematoxylin and eosin and Oil Red-O staining), 12 patients were classified into the NAFL group, 19 into the NASH group, and 5 into the control (non-NAFLD) group. Biochemical characterization of patient plasma was followed by expression analysis of genes regulating inflammation and lipid metabolism. The MCPIP1 protein level was reduced in the livers of NAFL and NASH patients in

Abbreviations: ACC1, Acetyl-CoA carboxylase 1; ACOX1, Acyl-CoA Oxidase 1; AKT, Protein kinase B; ALT, alanine aminotransferase; AST, aspartate aminotransferase; BMI, body mass index; C/EBPβ, CCAAT/enhancer-binding protein; CCL2, C-C Motif Chemokine Ligand 2; CPT1a, Carnitine Palmitoyltransferase 1A; CXCL11, C-X-C motif chemokine 11; EDTA, ethylenediaminetetraacetic acid; FAS, Fatty Acid Synthase; GTTP, Gamma-glutamyl Transpeptidase; HBV, hepatitis virus B; HCV, hepatitis virus C; HFD, high fat diet; HIV, human immunodeficiency virus; IFNγ, interferon gamma; IGF-1R, Insulin-like Growth Factor 1 Receptor; IL, interleukin; IQR, interquartile range; IR, Insulin Receptor; LCN2, Lipocalin-2; MCPIP1, Monocyte Chemotactic Protein-1-Induced Protein-1; MED, median;NAFLD, Non-alcoholic fatty liver disease; NAFL, Non-alcoholic fatty liver; NASH, Non-alcoholic steatohepatits; PBC, Primary Biliary Cholangitis; PBMCs, Peripheral blood mononuclear cells; PPAR, Peroxisome proliferator-activated receptor; SAT, subcutaneous adipose tissue; SREBP1, Sterol Regulatory Element-binding protein 1; TNF, Tumor Necrosis Factor; VAT, visceral adipose tissue.

Natalia Pydyn and Justyna Kadluczka are contributed equally as the first authors.

Supplemental Digital Content is available for this article. Direct URL citations appear in the printed text and are provided in the HTML and PDF versions of this article on the journal's website, www.hepcommjournal.com.

comparison to non-NAFLD control individuals. In addition, in all groups of patients, immunohistochemical staining showed that the expression of MCPIP1 was higher in the portal fields and bile ducts in comparison to the liver parenchyma and central vein. The liver MCPIP1 protein level negatively correlated with hepatic steatosis but not with patient body mass index or any other analyte. The MCPIP1 level in PBMCs did not differ between NAFLD patients and control patients. Similarly, in patients' PBMCs there were no differences in the expression of genes regulating β-oxidation (*ACOX1*, *CPT1A*, and *ACC1*) and inflammation (*TNF*, *IL1B*, *IL6*, *IL8*, *IL10*, and *CCL2*), or transcription factors controlling metabolism (*FAS*, *LCN2, CEBPB*, *SREBP1*, *PPARA*, and *PPARG*). **Conclusion:** We have demonstrated that MCPIP1 protein levels are reduced in NAFLD patients, but further research is needed to investigate the specific role of MCPIP1 in NAFL initiation and the transition to NASH.

INTRODUCTION

NAFLD is defined as the accumulation of excessive fat in the liver in the absence of excessive alcohol consumption and a lack of any secondary cause. Lipid accumulation in hepatocytes is a hallmark of the first stage of this disease and is called NAFL.[1] Although NAFL remission can be relatively easily achieved by lifestyle modifications and dietary changes, in ~25% of patients, the disease progresses to nonalcoholic steatohepatitis, hepatic fibrosis, liver cirrhosis, and hepatoma.[2] In addition to fat accumulation, the activation of liver-resident macrophages, together with the recruitment of monocytes, neutrophils, and lymphocytes into the liver parenchyma, is another hallmark of NASH. Both features have been associated with ongoing hepatic inflammation and NAFLD progression.[3]

The immune system plays a critical role in NAFLD progression; thus, the analysis of proteins that regulate inflammation may shed new light on the NAFL-to-NASH transition. One protein that negatively regulates the inflammatory reaction is monocyte chemoattractant protein-induced protein 1 (MCPIP1). MCPIP1 is an endoribonuclease that binds to the 3′ untranslated region fragments of mRNA and digests stem-loop structures. This endoribonuclease activity of MCPIP1 shortens the half-life of selected transcripts and therefore reduces the amount of protein expression.[4] Moreover, MCPIP1 is responsible for the degradation of translationally active transcripts and is particularly important in the initial stage of inflammation.[5] It was also shown that MCPIP1 inhibits the maturation of pre-miRNAs by digestion of hairpin structures, which leads to a reduction in the miRNA cellular pool.[6] The anti-inflammatory properties of MCPIP1 have also been confirmed *in vivo*. Mcpip1 knockout mice spontaneously develop a systemic inflammatory response that leads to splenomegaly, lymphadenopathy, and hyperimmunoglobulinemia and ultimately leads to death within 12 weeks.[7]

Mcpip1 acts as an important regulator of liver homeostasis both in mice fed chow and high-fat diet.[8] In addition, its deletion in murine liver epithelial cells recapitulates the features of primary biliary cholangitis (PBC), which manifests as excessive proliferation of intrahepatic bile ducts, bile duct destruction, inflammatory infiltration, and fibrosis.[9] Sun et al.[10] described a protective role of Mcpip1 in liver recovery after ischemia/reperfusion injury. Mcpip1 ameliorates liver damage, reduces inflammation, prevents cell death, and promotes tissue regeneration.

Despite data from mouse models, the functions of MCPIP1 in the human liver are still not known. Thus, in the current study, the MCPIP1 protein level was analyzed in a cohort of 36 patients who were divided into non-NAFLD, NAFL, or NASH groups based on liver histological analysis according to NAFLD Activity Score grading. For the first time, we demonstrated the diminished expression of MCPIP1 in the livers of NAFL and NASH patients in comparison to non-NAFLD control individuals. In addition, the analysis of MCPIP1 distribution in liver tissue by immunohistochemical staining showed lower levels of MCPIP1 expression in the parenchyma and central vein than in the portal fields and bile ducts.

MATERIALS AND METHODS

Collection of blood and liver samples

Samples were collected from 36 patients [24 female and 12 male, body mass index (BMI) ranged from 36 to 70] who underwent bariatric surgery in The Second Department of General Surgery, Jagiellonian University Medical College

(Krakow, Poland). Exclusion criteria included HCV/HBV/HIV infection, autoimmune diseases, cancer, and alcohol abuse. Of 36 patients, 15 were diabetic. Patients who were hospitalized due to a primary inguinal hernia and qualified for laparoscopic transabdominal preperitoneal repair were enrolled in the non-NAFLD group. Blood for the analysis of blood count, plasma biochemistry, and isolation of peripheral blood mononuclear cells (PBMCs) was collected from fasting patients before bariatric surgery. Liver samples were acquired during bariatric surgery. One liver sample was placed in formalin (for histological analysis). The second liver sample was snap-frozen in liquid nitrogen and then stored at −80°C (for protein analysis). All human tissue samples were collected according to the established protocol approved by the Local Bioethics Committee (approval no. 122.6120.263.2016). All subjects provided written consent for the study. All research was conducted in accordance with both the Declarations of Helsinki and Istanbul.

Blood analysis

All blood tests were measured routinely on the day of admission to the hospital in University Hospital laboratories with ISO 9001 certificates, using comparable laboratory methods.

Isolation of PBMCs

Ten milliliters of EDTA-anticoagulated blood was collected from each patient and transferred to 15 mL tubes. In the first stage, blood was centrifuged at 400*g* for 10 minutes, and the plasma was removed. Then, the remaining blood was replenished with PBS to a volume of 10 mL and layered on top of 5 mL of Ficoll solution (1.077 g/mL). Gradients were centrifuged at 400*g* for 30 minutes at room temperature in a swinging-bucket rotor without the brake applied. The layer of mononuclear cells was collected and washed twice with PBS by centrifugation. Finally, the cells were counted and suspended in appropriate buffers for RNA or protein extraction. Approximately 10^7 cells were obtained from each patient.

Protein isolation and western blot

PBMCs from patients were lysed using RIPA buffer (25 mM Tris-HCl, pH 7.6; 150 mM NaCl; 1% sodium deoxycholate; 0.1% SDS) supplemented with Complete Protease Inhibitor Cocktail (Roche) and PhosSTOP Phosphatase Inhibitor Cocktail (Roche). A bicinchoninic acid assay was used to assess the protein concentrations. Liver samples from patients were lysed in whole cell lysis buffer (62.5 mM Tris-HCl, pH 6.8; 2% SDS; 25% glycerol; 5% β-mercaptoethanol) supplemented with Complete Protease Inhibitor Cocktail (Roche) and PhosSTOP Phosphatase Inhibitor Cocktail (Roche). NanoDrop 1000 Spectrophotometer (Thermo Fisher Scientific) was used to assess the protein concentrations. Then, 50 μg of protein was separated on a 10% SDS-PAGE polyacrylamide gel. After wet transfer onto polyvinylidene fluoride membranes (Millipore), the membranes were blocked in 5% skim milk and then incubated with primary antibodies at 4°C overnight. On the following day, the membranes were washed and incubated with a secondary antibody for 1 hour at room temperature. Chemiluminescence was detected after 5 minutes of incubation with ECL Select Western Blotting Detection Reagent (GE Healthcare) in a ChemiDoc chemiluminescence detector (BioRad). The following antibodies were used: rabbit anti-MCPIP1 (1:2000; GeneTex), mouse anti-β-actin (1:4000; Sigma), rabbit anti-p-IGF1R$^{Tyr1135/1136}$/IRTyr$^{1150/1151}$ (1:1000; Cell Signaling), rabbit anti-IR (1:1000; Cell Signaling), anti-p-Akt^{Ser473} (1:1000; Cell Signaling), rabbit anti-IGF-1R (1:2000; Cell Signalling), rabbit anti-Akt (1:1000 Cell Signalling), rabbit anti-PPARγ (1:1000; Cell Signaling), rabbit anti-PPARα (1:1000 GeneTex), peroxidase-conjugated anti-rabbit (1:30,000; Cell Signaling) and peroxidase-conjugated anti-mouse (1:20,000; BD).

RNA isolation and real-time PCR

Total RNA from PBMCs was isolated using Fenozol (A&A Biotechnology). A NanoDrop 1000 Spectrophotometer (Thermo Fisher Scientific) was used to assess the RNA concentration and quality. For reverse transcription, 1 μg of total RNA, oligo(dT) primer (Promega), and M-MLV reverse transcriptase (Promega) were used. Real-time PCR was carried out using Sybr Green Master Mix (A&A Biotechnology) and QuantStudio Real-Time PCR System (Applied Biosystems). Gene expression was normalized to elongation factor-2 (EF2), and then, the relative transcript level was quantified by the $2^{-\Delta C_t}$ method. The primer sequences (Genomed/Sigma) and annealing temperatures are listed in Table S1 (Supplementary Material, http://links.lww.com/HC9/A32).

Histological analysis

Livers were fixed in 4% buffered formalin. Afterwards, tissue fragments were divided into 2 parts. One piece was immersed in a 30% sucrose solution overnight for cryoprotection and then frozen in Tissue-Tek OCT medium at −80°C. Frozen sections were stained using the Oil Red-O (ORO) method for fat deposition and photographed under 100× magnification. Ten images of each section were randomly obtained and subsequently analyzed by the Columbus Image Data Storage and Analysis System (Perkin Elmer) with an algorithm adapted for Oil Red-O stained sections. The second

piece was processed using standard paraffin procedures, and 5-μm paraffin tissue sections were stained with hematoxylin and eosin and then visualized using a standard light microscope (Olympus BX51; Olympus Corporation). Immunohistochemical MCPIP1 staining was performed using a primary anti-MCPIP1 antibody (1:200; Genetex) and EnVision Detection Systems Peroxidase/DAB, Rabbit/Mouse (Dako).

Histopathological analyzes were performed by 2 independent experimental pathologists in a blinded way. Histopathological assessments and microphoto documentation were made using a Axiolab A5 light microscope with Axiocam 208 color and ZEN 3.0 software (Zeiss). NAFLD activity score was used to assess the severity of changes in the liver. Measurements of the MCPIP1 immunoexpression in the liver was performed by measuring the optical density in the ImigeJ software and the ZEN software (Zeiss). Measurements were made on photos taken under the ×40 lens magnification for histological structures such as bile ducts, portal venous and lymphatic vessels, central veins, hepatocytes in zones I and III of hepatic lobules. For each of the indicated structures, 35 measurements were made for each sample.

Statistical analysis

The results are expressed as the median ± interquartile range (IQR). Nonparametric 1-way ANOVA with Tukey's posttest for multiple comparisons was performed using GraphPad Prism software. For analyses of correlations, the Pearson correlation coefficient was used. The p values are marked with asterisks in the charts (*$p < 0.05$; **$p < 0.01$; ***$p < 0.001$).

RESULTS

Morphological and biochemical characterization of the patients

In the following study, we analyzed a cohort of 36 patients (24 women and 12 men) who underwent operation at the Collegium Medicum Jagiellonian University and were diagnosed according to the European Association for the Study of the Liver. Based on hematoxylin and eosin and Oil Red-O staining, patients were divided into non-NAFLD (n = 5), NAFL (n = 12), and NASH (n = 19) groups (Figure 1C and Figures S1, http://links.lww.com/HC9/A26, S2, http://links.lww.com/HC9/A27). The baseline characteristics of the analyzed groups are summarized in (Table 1) and Table S2 (http://links.lww.com/HC9/A33). Blood morphology analysis showed that all patients had elevated levels of white blood cells, monocytes, and neutrophils; however, there were no significant differences among the groups (Table S2, http://links.lww.com/HC9/A33). Patients in all groups were hyperglycemic, with increased aspartate aminotransferase and alanine aminotransferase activity (Table 1). In comparison to non-NAFLD group, the NAFL and NASH groups demonstrated increased BMI, urea concentrations, and gamma-glutamyl transpeptidase activity (Table 1).

Analysis of MCPIP1 liver levels and tissue-specific distribution

The MCPIP1 protein level in the liver was significantly lower in NAFL (median = 1.86, IQR: 0.90–2.58) and NASH patients (median = 2.03, IQR: 1.33–2.45) than in non-NAFLD control individuals (median = 4.18 IQR: 2.31–5.71) (Figure 1A and Figure S3A, http://links.lww.com/HC9/A28). We have previously shown that MCPIP1 is a potent inhibitor of adipogenesis and that its level in adipose tissue inversely correlates with patients' BMI.[11,12] Thus, in the next step, we analyzed the amount of MCPIP1 protein in the patients' livers in relation to hepatic steatosis and BMI. As shown in (Figure 1), the MCPIP1 level was inversely correlated with hepatic steatosis ($r^2 = 0.587$; Figure 1B) but not with BMI (Figure S3B, http://links.lww.com/HC9/A28). Finally, analysis of cellular MCPIP1 localization revealed that its level was the lowest in the central vein and in the liver parenchyma (both in centrilobular and perilobular hepatocytes) (Figure 2). In addition, in all patient groups, the MCPIP1 level was the highest in bile duct epithelial cells (cholangiocytes) and in lymphatic and blood vessels in the portal area (Figure 2).

Evaluation of insulin signaling and metabolic signaling in the livers of NAFLD patients

The hepatic levels of insulin receptor (IR) were reduced in NAFL patients (median = 0.30, IQR: 0.13–0.53) in comparison to the non-NAFLD patients (median = 0.96, IQR: 0.36–1.36); however, there was no difference in its phosphorylation (Figure 3A, B and Figure S4, http://links.lww.com/HC9/A29). Similarly, the protein level of insulin-like growth factor 1 receptor (IGF-1R) was significantly reduced in the NAFL cohort (median = 0.17, IQR: 0.01–0.39) compared with the non-NAFLD cohort (median = 0.73, IQR: 0.36–1.13), without differences in its phosphorylation (Figure 3C, D and Figure S4, http://links.lww.com/HC9/A29). In addition, NAFL patients had a diminished amount of protein kinase B (AKT) (median = 0.52, IQR: 0.29–0.72) when compared to non-NAFLD patients (median = 1.21, IQR: 0.62–1.89), but this was not observed for its phosphorylated form (Figure 3E, F and Figure S4, http://links.lww.com/HC9/A29). Patients from the NASH group had only a reduced amount of IGF-1R levels (median = 0.32, IQR: 0.24–0.45) in comparison

TABLE 1 Clinical and laboratory characteristics of patients

	Non-NAFLD (N = 5)	NAFL (N = 12)	NASH (N = 19)
Age (years)	41 (37–47)	41 (35–49)	45 (41–51)
Sex			
Female/male	4/1	7/5	13/6
BMI			
18.50–24.99	26.8 (23.8–48.2)	47.4 (40.3–54.9)[a]	47.0 (39.3–51.7); ***p* = 0.09**
Sodium			
136–145 mmol/L	138 (137–140)	141 (138–142)	141 (139–142)
Potassium			
3.5–5.1 mmol/L	4.17 (3.79–4.60)	4.24 (4.17–4.46)	4.14 (4.03–4.47)
Iron			
5.83–34.5 μmol/L	8.40 (5.43–10.30)	9.27 (7.78–10.92)	8.58 (6.26–9.54)
Glucose			
3.3–5.6 mmol/L	**5.65 (5.43–8.08)**	**6.10 (5.36–6.82)**	**6.41 (5.73–8.41)**
HbA1c			
4.3%–5.9%	5.7 (5.3–7.3)	5.7 (5.3–6.3)	**6.0 (5.7–7.5)**
Bilirubin			
0–21 μmol/L	7.0 (6.4–11.6)	10.0 (8.4–13.5)	10.4 (8.2–14.2)
Urea			
2.76–8.07 mmol/L	2.8 (2.4–3.5)	5.0 (3.7–5.5)[a]	3.8 (3.5–5.1)[a]
Creatinine			
44–106 μmol/L	69 (56–86)	73 (59–85)	74 (65–94)
Total protein			
66–87 g/L	69.2 (60.8–74.9)	70.4 (61.0–73.6)	67.0 (62.3–69.6)
Albumins			
35–52 g/L	41.6 (34.8–45.5)	43.2 (38.1–45.2)	41.9 (37.9–43.5)
Cholesterol			
3.2–5.2 mmol/L	4.4 (4.1–4.9)	4.2 (3.9–4.9)	3.8 (3.3–4.5)
HDL			
> 1.2 mmol/L	1.23 (1.09–1.73)	**1.19 (0.87–1.45)**	**1.16 (1.05–1.29)**
LDL			
< 3.4 mmol/L	2.45 (2.10–3.01)	2.45 (2.26–2.74)	2.37 (1.41–2.90)
Triglycerides			
< 2.26 mmol/L	1.51 (0.85–2.18)	1.31 (1.10–2.06)	1.31 (1.13–1.84)
AST			
5–40 U/L	**51 (31–104)**	**48 (43–94)**	**82 (62–112)**
ALT			
5–41 U/L	**62 (33–157)**	**65 (47–139)**	**91 (78–114)**
GTTP			
5–61 U/L	10 (8–18)	29 (24–39)[a]	29 (23–58)[b]
ALP			
35–129 U/L	61 (55–88)	59 (50–65)	66 (50–73)
Cholinesterase			
5320–12,921 U/L	7313 (6463–7693)	7746 (6872–8798)	7604 (6924–8746)
Ferritin			
13–400 U/L	60 (37–78)	232 (88–650)[a]	125 (87–202)

Data are presented as median (interquartile range) with abnormal values marked in bold and reference values shown in italics. Data were compared using 1-way ANOVA with Tukey's posttest.

Abbreviations: ALP, alkaline phosphatase; ALT, alanine aminotransferase; AST, aspartate aminotransferase; BMI, body mass index; GTTP, gamma-glutamyl transpeptidase; HbA1c, hemoglobin A1c.

[a] $p < 0.05$.

[b] $p < 0.01$ versus non-NAFLD group.

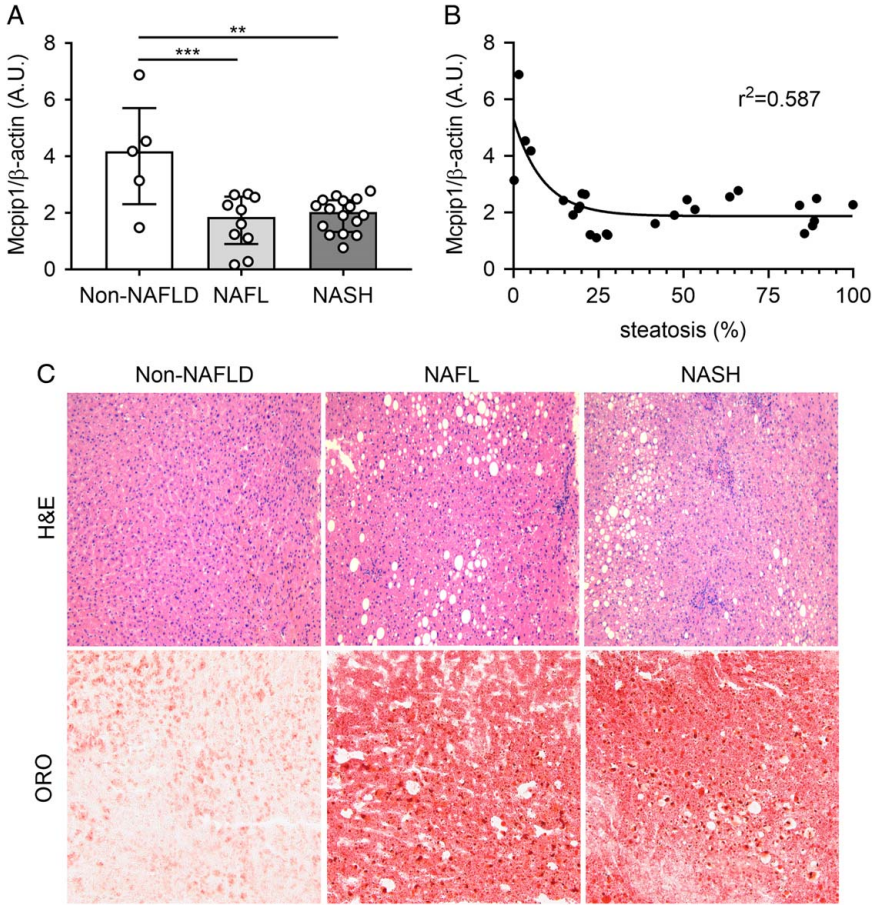

FIGURE 1 The MCPIP1 level is reduced in the livers of NAFL and NASH patients. (A) Densitometric quantification of MCPIP1 protein levels in the livers of control subjects, NAFL patients, and NASH patients. (B) Correlation between liver MCPIP1 protein levels and % of liver steatosis (% of tissue area stained with lipids). (C) Representative hematoxylin and eosin and Oil Red-O staining of livers from non-NAFLD, NAFL, and NASH patients. Statistical significance was determined with the Pearson correlation. Data were compared using 1-way ANOVA with Tukey's posttest. The graphs show the median ± interquartile range. $^{**}P < 0.01$; $^{***}P < 0.001$.

to non-NAFLD group (median = 0.73, IQR: 0.36–1.13) (Figure 3 and Figure S4, http://links.lww.com/HC9/A29).

Finally, there was a tendency for higher protein levels of peroxisome proliferator-activated receptor alpha (PPARα) in the livers of non-NAFLD patients (median = 0.71, IQR: 0.14–1.27) than in both NAFL (median = 0.08, IQR: 0.01–0.14) and NASH patients (median = 0.25, IQR: 0.14–0.59) (Figure 3G and Figure S4, http://links.lww.com/HC9/A29). There was no difference in the expression of a second nuclear receptor, namely peroxisome proliferator-activated receptor gamma (PPARγ) (Figure 3H and Figure S4, http://links.lww.com/HC9/A29).

Level of expression of MCPIP1 in PBMCs inversely correlates with patient BMI

We have recently demonstrated that the deletion of Mcpip1 in myeloid leukocytes in mice leads to dyslipidemia, low plasma glucose levels, and proinflammatory phenotypes that impact NAFLD development.[8] However, in the current study, we showed that the MCPIP1 levels in PBMCs from humans did not differ among non-NAFLD, NAFL, and NASH patients (Figure 4A), but they were negatively correlated with patient BMI ($p = 0.018$; $r^2 = 0.198$; Figure 4B, D) and CEBP/β transcript levels ($p = 0.025$; $r^2 = 0.249$; Figure 4C).

Next, we determined the expression levels of key genes that regulate β-oxidation (*ACOX1*, *CPT1A*, and *ACC1*) and inflammation (*TNF*, *IL1B*, *IL6*, *IL8*, *IL10*, and *CCL2*) and transcription factors that control metabolism (*FAS*, *LCN2*, *CEBPB*, *SREBP1*, *PPARA*, and *PPARG*) in PBMCs patients. None of these genes were differentially expressed between non-NAFLD patients and the NAFL or NASH groups (Figure 4E, F and Figure S5, http://links.lww.com/HC9/A30).

DISCUSSION

In the present study, we have shown that MCPIP1 levels are reduced in liver biopsies collected from NAFLD patients, including both NAFL and NASH patients, in comparison to non-NAFLD control

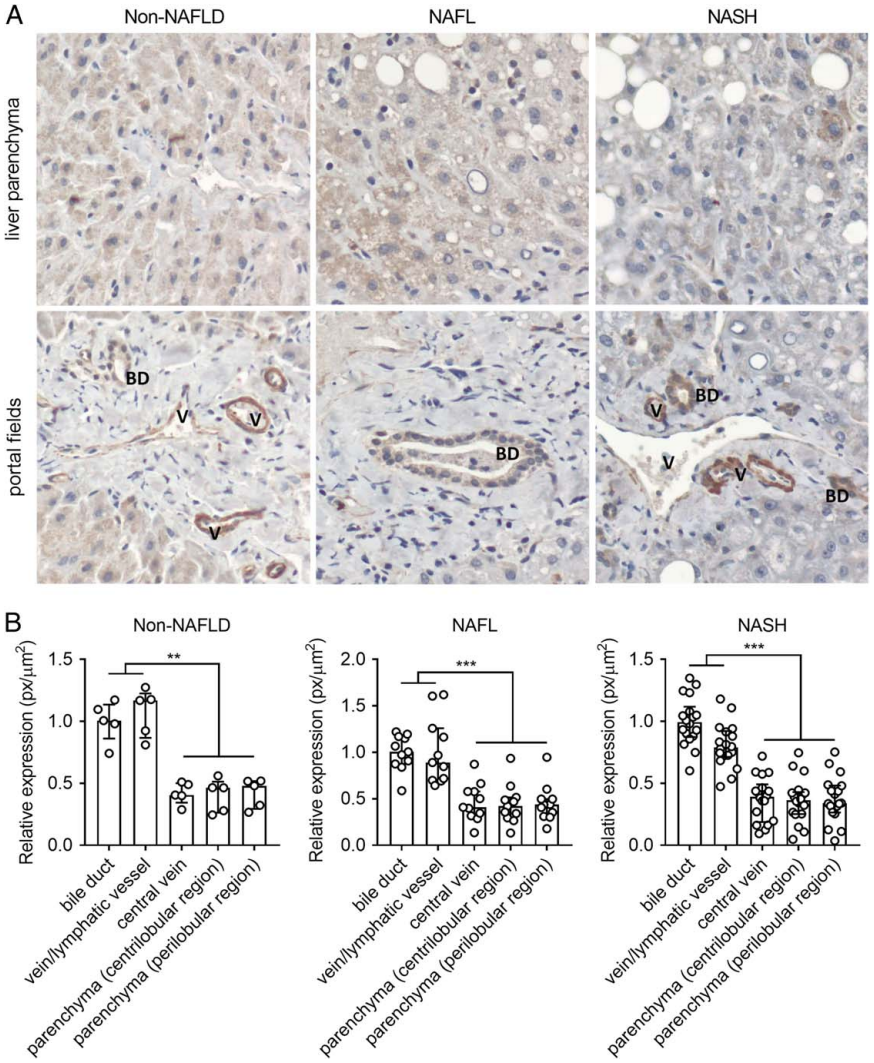

FIGURE 2 Liver MCPIP1 is predominantly present in bile ducts (BD), veins (V), and lymphatic vessels. (A) Representative immunohistochemical staining of MCPIP1 in liver parenchyma and portal fields. (B) Quantitative analysis of MCPIP1 levels in distinct liver areas in non-NAFLD, NAFL, and NASH patients. Data were compared using 1-way ANOVA with Tukey's posttest. The graphs show the median ± interquartile range. $^{**}P < 0.01$; $^{***}P < 0.001$.

individuals. The possible link between NAFLD and MCPIP1 results from its involvement in lipid metabolism and the regulation of inflammation, as both processes are hallmarks of NAFLD development and progression. MCPIP1 plays an important role in the inhibition of adipogenesis by direct degradation of CCAAT/enhancer binding protein beta (C/EBPβ) transcript.[11] Moreover, ectopic overexpression of MCPIP1 in differentiating mouse preadipocytes impaired adipogenesis not only by the direct cleavage of C/EBPβ mRNA but also by modulating the cellular miRNA pool.[13] In addition, Mcpip1 levels were lower in primary hepatocytes isolated from high-fat diet-fed mice than in control cells, and thus, it possibly functions to facilitate hepatic lipid accumulation. In addition, the expression level of Mcpip1 was depleted in visceral fat isolated from obese and glucose-intolerant mice characterized by fatty liver disease in comparison to lean controls.[8]

To date, there is only one report describing MCPIP1 levels in patients afflicted with obesity.[12] Losko et al.[12] analyzed MCPIP1 expression in biopsies of subcutaneous and visceral adipose tissue of lean and obese subjects with body mass indices ranging from 27 to 57. In both subcutaneous and visceral, there was a correlation between the MCPIP1 protein level and BMI, as decreased protein levels of MCPIP1 correlated with increased BMI. We found a similar correlation between MCPIP1 levels in PBMCs and BMI, but this correlation was not observed for the expression levels of MCPIP1 in the liver. In addition, in PBMCs, the level of MCPIP1 protein was inversely correlated with the C/EBPβ transcript, which might be explained by the direct degradation of C/EBPβ mRNA by this RNase.[14]

One of the key master regulators of liver metabolism is PPARα, which is a ligand-activated transcription factor. PPARα regulates the expression of genes involved in fatty

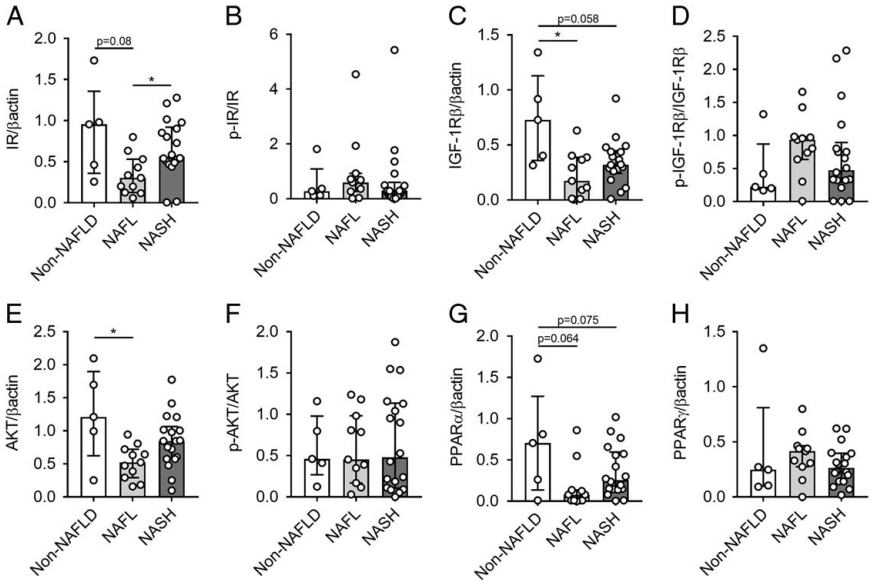

FIGURE 3 Liver IR, IGF-1Rβ, AKT, and PPARα protein levels are decreased in NAFLD patients. Densitometric quantification of insulin receptor (IR) (A), p-IR (B), insulin-like growth factor 1 receptor beta (IGF-1Rβ) (C), p-IGF-1Rβ (D), protein kinase B (AKT) (E), p-AKT (F), peroxisome proliferator-activated receptor alpha (PPARα) (G), and peroxisome proliferator-activated receptor gamma (PPARγ) protein (H) levels in the livers of control subjects, NAFL patients and NASH patients. Data were compared using 1-way ANOVA with Tukey's posttest. The graphs show the median ± interquartile range. $*P < 0.05$.

acid uptake, beta-oxidation, ketogenesis, bile acid synthesis, and triglyceride turnover and thus plays a critical role in the control of metabolism.[15] PPARα deficiency leads to excessive lipid accumulation in the liver, resulting in spontaneous steatosis in mice fed a chow diet.[16] Moreover, PPARα deficiency promotes NAFLD and liver inflammation in mice fed a high fat diet.[17] In humans with NAFLD, hepatic expression of PPARα is decreased, which is in line with our observations.[18] Interestingly, PPARα levels were also found to increase in parallel with NAFLD histological improvements secondary to lifestyle intervention or bariatric surgery.[15,18] In addition, pharmacological activation of PPARα with fenofibrate, gemfibrozil, or bezafibrate has beneficial effects in NAFLD patients.[19–21]

MCPIP1 cleaves RNA molecules to regulate a plethora of cellular processes, such as inflammation, cellular differentiation, angiogenesis, and adipogenesis.[11,22–24] By direct degradation of transcripts encoding proinflammatory cytokines (e.g., IL-1β, IL-6, and IL-8),[5,25] MCPIP1 tightly controls the immune system. A constitutive deletion of Mcpip1 in mice leads to a lethal phenotype resulting from severe systemic and multiorgan inflammation.[7] Mcpip1 deletion in mice was also shown to trigger autoimmune diseases, such as gastritis (whole-body Mcpip1 knockout),[26] lupus (deletion in myeloid leukocytes),[27] and primary biliary cholangitis (deletion in liver epithelial cells).[9]

Our results show the cellular distribution of the MCPIP1 protein in human livers and highlight its important role in the biology of cholangiocytes and endothelial cells, where the MCPIP1 level was the highest in all experimental groups. In line with these immunohistochemistry data, both the Human Protein Atlas and Liver Single Cell Atlas demonstrate cholangiocytes as a population with the highest *ZC3H12A* expression in comparison to other liver cells (https://www.proteinatlas.org/[28]). The Liver Single Cell Atlas was generated by Brancale and Vilarinho, who integrated and analyzed available human liver single-cell RNA sequencing datasets. The authors used results from gene expression data across a variety of annotated parenchymal and nonparenchymal cells derived from 28 healthy human livers analyzed by 5 independent studies. In addition to cholangiocytes, a high level of *ZC3H12A* was also detected in lymphoid cells and in hepatocytes.[28] Finally, Mcpip1 deficiency in murine liver epithelial cells leads to the development of PBC symptoms. Thus, it would be interesting to analyze *ZC3H12A* expression in the livers from PBC patients and tumors collected from cholangiocarcinoma and hepatocellular carcinoma biopsies.

Although liver biopsy is still the gold standard for NAFLD assessment, a less invasive collection of liquid biopsy involving blood sampling is highly appreciated. Thus, a liquid biopsy containing PBMCs, extracellular vehicles, or circulating DNA might be used as a diagnostic and monitoring tool. PBMCs are widely used as screening materials for the identification of new disease-associated biomarkers. They can reflect the gene expression profile involved in a number of pathological conditions, including obesity, inflammation, or oxidative stress.[29,30] Importantly, they express receptors for insulin, glucagon, and leptin on their surface, and thus they can respond to hormonal changes that reflect

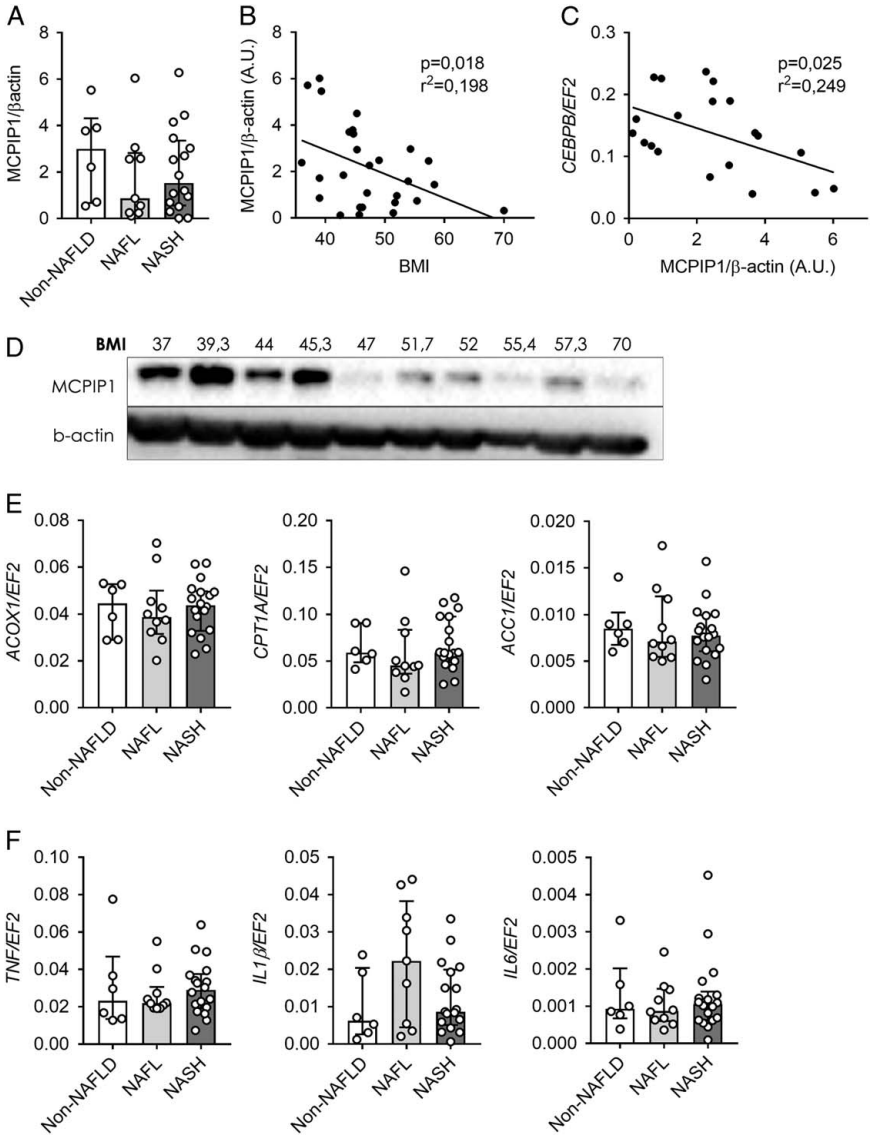

FIGURE 4 The MCPIP1 level in peripheral blood mononuclear cells (PBMCs) negatively correlates with patient body mass index (BMI). (A) Densitometric quantification of MCPIP1 protein levels in PBMCs of control subjects, NAFL patients, and NASH patients. (B) Correlation between BMI and MCPIP1 protein levels in PBMCs. (C) Correlation between MCPIP1 protein levels in PBMCs and C/EBPβ mRNA. (D) Representative western blot showing the correlation between MCPIP1 protein levels and patient BMI. Expression of *ACOX1*, *CPT1A*, and *ACC1* (E) and *TNF*, *IL-1β*, and *IL-6* (F) genes in PBMCs of control subjects, NAFL patients, and NASH patients. Data were compared using 1-way ANOVA with Tukey's posttest. Statistical significance was determined with Pearson correlation. The graphs show the median ± interquartile range.

the metabolic response of various organs.[31,32] Moreover, the human MCPIP1 transcript was originally shown to be highly expressed in leukocytes.[33] The PBMC expression profile might also be used for discriminating NASH from NAFL patients because the expression levels of cytokine-encoding and chemokine-encoding genes (interferon γ, IL-2, IL-15, CCL2, CXCL11, and IL-10) in PBMCs were significantly upregulated in PBMCs from NASH patients in comparison to those from NAFL patients.[34] Although the expression of genes regulating β-oxidation, inflammation and controlling metabolism selected by us did not differ in these cohorts of NAFL and NASH patients, Kado et al.[34] were able to successfully divide most of 54 NAFLD patients into NAFL and NASH groups based on interferon γ, CCL2, and IL-10 expression levels. It is also possible to use flow cytometry analysis of blood leukocytes to discriminate NAFL and NASH patients. Both peripheral lymphocyte and myeloid cell subsets differ in terms of their abundance, activation, polarization, or cell membrane markers.[35,36]

Taken together, our data demonstrate that the MCPIP1 protein level is reduced in the livers of NAFL and NASH patients and is predominantly expressed in cholangiocytes, veins, and lymphatic vessels. Our data also revealed that the amount of PPARα was reduced in NAFLD patients, which is in agreement with

recent studies. Although the MCPIP1 level in PBMCs was not affected by NAFLD, its level correlated with patients' BMI and C/EBPβ transcript level. Further research is required to investigate the specific role of MCPIP1 in both NAFL initiation and the transition to NASH. Such experiments might be performed, for example, on tissue-specific Mcpip1 knockout mouse models subjected to diet-induced obesity or sterile inflammation.

ACKNOWLEDGMENTS

The authors thank Agnieszka Jasztal, Edyta Kus, and Stefan Chlopicki from Jagiellonian Centre for Experimental Therapeutics at Jagiellonian University for excellent help with liver histology staining.

CONFLICT OF INTEREST

Nothing to report.

ETHICAL APPROVAL

All human tissue samples were collected according to the established protocol approved by the Local Bioethics Committee (approval no. 122.6120.263.2016).

PATIENT CONSENT STATEMENT

All subjects provided consent for the study.

ORCID

Natalia Pydyn http://orcid.org/0000–0002–9145–1979
Justyna Kadluczka http://orcid.org/0000–0002–2341–2994
Piotr Major http://orcid.org/0000–0001–6552–7979
Tomasz Hutsch http://orcid.org/0000–0001–6491–3800
Kinga Belamri http://orcid.org/0000–0001–8698–3068
Piotr Malczak http://orcid.org/0000–0002–2142–7121
Dorota Radkowiak http://orcid.org/0000–0002–8158–6116
Andrzej Budzynski http://orcid.org/0000–0003–3021–6470
Katarzyna Miekus http://orcid.org/0000–0002–2716–203X
Jolanta Jura http://orcid.org/0000–0002–0816–3475
Jerzy Kotlinowski http://orcid.org/0000–0002–3133–3364

REFERENCES

1. Estes C, Anstee QM, Arias-Loste MT, Bantel H, Bellentani S, Caballeria J, et al. Modeling NAFLD disease burden in China, France, Germany, Italy, Japan, Spain, United Kingdom, and United States for the period 2016–2030. J Hepatol. 2018;69:896–904.
2. Pydyn N, Mięk̨us K, Jura J, Kotlinowski J. New therapeutic strategies in nonalcoholic fatty liver disease: a focus on promising drugs for nonalcoholic steatohepatitis. Pharmacol Rep. 2020;72:1–12.
3. Singh S, Allen AM, Wang Z, Prokop LJ, Murad MH, Loomba R. Fibrosis progression in nonalcoholic fatty liver versus nonalcoholic steatohepatitis: a systematic review and meta-analysis of paired-biopsy studies. Clin Gastroenterol Hepatol. 2015;13:643–54.
4. Musson R, Szukała W, Jura J. MCPIP1 RNase and Its Multifaceted Role. Int J Mol Sci. 2020;21:7183.
5. Mino T, Murakawa Y, Fukao A, Vandenbon A, Wessels HH, et al. Regnase-1 and roquin regulate a common element in inflammatory mRNAs by spatiotemporally distinct mechanisms. Cell. 2015;161:1058–73.
6. Suzuki H, Arase M, Matsuyama H, Choi YL, Ueno T, Mano H, et al. MCPIP1 ribonuclease antagonizes dicer and terminates microRNA biogenesis through precursor microRNA degradation. Mol Cell. 2011;44:424–36.
7. Liang J, Saad Y, Lei T, Wang J, Qi D, Yang Q, et al. MCP-induced protein 1 deubiquitinates TRAF proteins and negatively regulates JNK and NF-kappaB signaling. J Exp Med. 2010;207:2959–73.
8. Pydyn N, Żurawek D, Kozieł J, Kus E, Wojnar-Lason K, Jasztal A, et al. Role of Mcpip1 in obesity-induced hepatic steatosis as determined by myeloid and liver-specific conditional knockouts. FEBS J. 2021;288:6563–80.
9. Kotlinowski J, Hutsch T, Czyzynska-Cichon I, Wadowska M, Pydyn N, Jasztal A, et al. Deletion of Mcpip1 in Mcpip1$^{fl/fl}$Alb^{Cre} mice recapitulates the phenotype of human primary biliary cholangitis. Biochim Biophys Acta Mol Basis Dis. 2021;1867:166086.
10. Sun P, Lu YX, Cheng D, Zhang K, Zheng J, Liu Y, et al. Monocyte chemoattractant protein-induced protein 1 targets hypoxia-inducible factor 1α to protect against hepatic ischemia/reperfusion injury. Hepatology. 2018;68:2359–75.
11. Lipert B, Wegrzyn P, Sell H, Eckel J, Winiarski M, Budzynski A, et al. Monocyte chemoattractant protein-induced protein 1 impairs adipogenesis in 3T3-L1 cells. Biochim Biophys Acta. 2014;1843:780–8.
12. Losko M, Dolicka D, Pydyn N, Jankowska U, Kedracka-Krok S, Kulecka M, et al. Integrative genomics reveal a role for MCPIP1 in adipogenesis and adipocyte metabolism. Cell Mol Life Sci. 2020;77:4899–919.
13. Losko M, Lichawska-Cieslar A, Kulecka M, Paziewska A, Rumienczyk I, Mikula M, et al. Ectopic overexpression of MCPIP1 impairs adipogenesis by modulating microRNAs. Biochim Biophys Acta Mol Cell Res. 2018;1865:186–95.
14. Lipert B, Wilamowski M, Gorecki A, Jura J. MCPIP1, alias Regnase-1 binds and cleaves mRNA of C/EBPβ. PLoS One. 2017;12:e0174381.
15. Pawlak M, Lefebvre P, Staels B. Molecular mechanism of PPARα action and its impact on lipid metabolism, inflammation and fibrosis in non-alcoholic fatty liver disease. J Hepatol. 2015;62:720–33.
16. Montagner A, Polizzi A, Fouche E, Ducheix S, Lippi Y, et al. Liver PPARalpha is crucial for whole-body fatty acid homeostasis and is protective against NAFLD. Gut. 2016;65:1202–14.
17. Régnier M, Polizzi A, Smati S, Lukowicz C, Fougerat A, et al. Hepatocyte-specific deletion of Pparα promotes NAFLD in the context of obesity. Sci Rep. 2020;10:6489.
18. Francque S, Verrijken A, Caron S, Prawitt J, Paumelle R, Derudas B, et al. PPARalpha gene expression correlates with severity and histological treatment response in patients with non-alcoholic steatohepatitis. J Hepatol. 2015;63:164–73.
19. Fernandez-Miranda C, Perez-Carreras M, Colina F, Lopez-Alonso G, Vargas C, Solis-Herruzo JA. A pilot trial of fenofibrate for the treatment of non-alcoholic fatty liver disease. Dig Liver Dis. 2008;40:200–5.
20. Basaranoglu M, Acbay O, Sonsuz A. A controlled trial of gemfibrozil in the treatment of patients with nonalcoholic steatohepatitis. J Hepatol. 1999;31:384.
21. Nakamuta M, Morizono S, Soejima Y, Yoshizumi T, Aishima S, Takasugi S, et al. Short-term intensive treatment for donors with hepatic steatosis in living-donor liver transplantation. Transplantation. 2005;80:608–12.

22. Matsushita K, Takeuchi O, Standley DM, Kumagai Y, Kawagoe T, Miyake T, et al. Zc3h12a is an RNase essential for controlling immune responses by regulating mRNA decay. Nature. 2009;458: 1185–90.
23. Wang K, Niu J, Kim H, Kolattukudy PE. Osteoclast precursor differentiation by MCPIP via oxidative stress, endoplasmic reticulum stress, and autophagy. J Mol Cell Biol. 2011;3:360–8.
24. Roy A, Zhang M, Saad Y, Kolattukudy PE. Antidicer RNAse activity of monocyte chemotactic protein-induced protein-1 is critical for inducing angiogenesis. Am J Physiol. 2015;305:C1021–32.
25. Dobosz E, Wilamowski M, Lech M, Bugara B, Jura J, Potempa J, et al. MCPIP-1, alias Regnase-1, controls epithelial inflammation by posttranscriptional regulation of IL-8 production. J Innate Immun. 2016;8:564–78.
26. Zhou Z, Miao R, Huang S, Elder B, Quinn T, Papasian CJ, et al. MCPIP1 deficiency in mice results in severe anemia related to autoimmune mechanisms. PLoS One. 2013;8: e82542.
27. Dobosz E, Lorenz G, Ribeiro A, Würf V, Wadowska M, Kotlinowski J, et al. Murine myeloid cell MCPIP1 suppresses autoimmunity by regulating B-cell expansion and differentiation. Dis Model Mech. 2021;14:dmm047589.
28. Brancale J, Vilarinho S. A single cell gene expression atlas of 28 human livers. J Hepatol. 2021;75:219–20.
29. Crujeiras AB, Parra D, Milagro FI, Goyenechea E, Larrarte E, Margareto J, et al. Differential expression of oxidative stress and inflammation related genes in peripheral blood mononuclear cells in response to a low-calorie diet: a nutrigenomics study. OMICS. 2008;12:251–61.
30. Caimari A, Oliver P, Keijer J, Palou A. Peripheral blood mononuclear cells as a model to study the response of energy homeostasis-related genes to acute changes in feeding conditions. OMICS. 2010;14:129–41.
31. Goldstein S, Blecher M, Binder R, Perrino PV, Recant L. Hormone receptors, 5. Binding of glucagon and insulin to human circulating mononuclear cells in diabetes mellitus. Endocr Res Commun. 1975;2:367–76.
32. Tsiotra PC, Pappa V, Raptis SA, Tsigos C. Expression of the long and short leptin receptor isoforms in peripheral blood mononuclear cells: implications for leptin's actions. Metabolism. 2000;49:1537–41.
33. Mizgalska D, Wegrzyn P, Murzyn K, Kasza A, Koj A, Jura J, et al. Interleukin-1-inducible MCPIP protein has structural and functional properties of RNase and participates in degradation of IL-1beta mRNA. FEBS J. 2009;276:7386–99.
34. Kado A, Tsutsumi T, Enooku K, Fujinaga H, Ikeuchi K, Okushin K, et al. Noninvasive diagnostic criteria for nonalcoholic steatohepatitis based on gene expression levels in peripheral blood mononuclear cells. J Gastroenterol. 2019;54:730–41.
35. Lin SZ, Fan JG. Peripheral immune cells in NAFLD patients: a spyhole to disease progression. EBioMedicine. 2022;75:103768.
36. Diedrich T, Kummer S, Galante A, Drolz A, Schlicker V, Lohse AW, et al. Characterization of the immune cell landscape of patients with NAFLD. PLoS One. 2020;15:e0230307.

How to cite this article: Pydyn N, Kadluczka J, Major P, Hutsch T, Wołoszyn K, Malczak P, et al. Hepatic MCPIP1 protein levels are reduced in NAFLD patients and are predominantly expressed in cholangiocytes and liver endothelium. Hepatol Commun. 2023;7:e0008. https://doi.org/10.1097/HC9.0000000000000008